AGU ADVANCING EARTH AND SPACE SCIENCE

Geophysical Research Letters

RESEARCH LETTER
10.1029/2022GL098586

High-Resolution Soil Moisture Data Reveal Complex Multi-Scale Spatial Variability Across the United States

Noemi Vergopolan[1,2,3], Justin Sheffield[4], Nathaniel W. Chaney[5], Ming Pan[6], Hylke E. Beck[7], Craig R. Ferguson[8], Laura Torres-Rojas[5], Felix Eigenbrod[4], Wade Crow[9], and Eric F. Wood[1]

[1]Department of Civil and Environmental Engineering, Princeton University, Princeton, NJ, USA, [2]Atmospheric and Ocean Sciences Program, Princeton University, Princeton, NJ, USA, [3]NOAA Geophysical Fluid Dynamics Laboratory, Princeton, NJ, USA, [4]School of Geography and Environmental Sciences, University of Southampton, Southampton, UK, [5]Department of Civil and Environmental Engineering, Duke University, Durham, NC, USA, [6]Center for Western Weather and Water Extremes, Scripps Institution of Oceanography, University of California, San Diego, CA, USA, [7]European Commission, Joint Research Centre (JRC), Ispra, Italy, [8]Atmospheric Sciences Research Center, University at Albany, State University of New York, Albany, NY, USA, [9]USDA Hydrology and Remote Sensing Laboratory, Beltsville, MD, USA

Abstract Soil moisture (SM) spatiotemporal variability critically influences water resources, agriculture, and climate. However, besides site-specific studies, little is known about how SM varies locally (1–100-m scale). Consequently, quantifying the SM variability and its impact on the Earth system remains a long-standing challenge in hydrology. We reveal the striking variability of local-scale SM across the United States using SMAP-HydroBlocks — a novel satellite-based surface SM data set at 30-m resolution. Results show how the complex interplay of SM with landscape characteristics and hydroclimate is primarily driven by local variations in soil properties. This local-scale complexity yields a remarkable and unique multi-scale behavior at each location. However, very little of this complexity persists across spatial scales. Experiments reveal that on average 48% and up to 80% of the SM spatial information is lost at the 1-km resolution, with complete loss expected at the scale of current state-of-the-art SM monitoring and modeling systems (1–25 km resolution).

Plain Language Summary Soil moisture (SM) widely varies in space and time. This variability critically influences freshwater availability, agriculture, ecosystem dynamics, climate and land-atmosphere interactions, and it can also trigger hazards such as droughts, floods, landslides, and aggravate wildfires. Limited SM observational data constrained our understanding of this variability and its impact on the Earth system. Here, we present the first continental assessment of how SM varies at the local scales using SMAP-HydroBlocks – the first 30-m surface SM data set over the United States. This study maps the SM spatial variability, characterizes the landscape drivers, and quantifies how this variability persists across larger spatial scales. Results revealed striking SM spatial variability across the United States, mainly driven by local spatial variations in soil properties and less so by vegetation and topography. However, this SM variability does not persist at coarser spatial scales resulting in extensive information loss. This information loss implicates inaccuracies when predicting non-linear SM-dependent hydrological, ecological, and biogeochemical processes using coarse-scale models and satellite estimates. By mapping the SM spatial variability locally and its scaling behavior, we provide a pathway toward understanding SM-dependent hydrological, biogeochemical, and ecological processes at local (and so far unresolved) spatial scales.

Key Points:

- 30-m soil moisture (SM) data shows striking and complex spatial variability driven mainly by climate and local variations in soil properties
- This variability yields a remarkable and unique multi-scale behavior at each location that cannot be generalized across the diverse US
- Up to 80% of SM information is lost at the 1-km scale, with complete loss at the scale of state-of-the-art SM observation/monitoring systems

Supporting Information:

Supporting Information may be found in the online version of this article.

Correspondence to:

N. Vergopolan,
noemi@princeton.edu

Citation:

Vergopolan, N., Sheffield, J., Chaney, N. W., Pan, M., Beck, H. E., Ferguson, C. R., et al. (2022). High-resolution soil moisture data reveal complex multi-scale spatial variability across the United States. *Geophysical Research Letters*, *49*, e2022GL098586. https://doi.org/10.1029/2022GL098586

Received 4 MAR 2022
Accepted 16 JUL 2022

Author Contributions:

Conceptualization: Noemi Vergopolan, Justin Sheffield
Formal analysis: Noemi Vergopolan
Funding acquisition: Justin Sheffield, Ming Pan, Eric F. Wood
Investigation: Noemi Vergopolan, Nathaniel W. Chaney, Ming Pan, Hylke E. Beck, Craig R. Ferguson, Laura Torres-Rojas
Methodology: Noemi Vergopolan, Justin Sheffield, Nathaniel W. Chaney, Ming Pan
Software: Noemi Vergopolan
Supervision: Eric F. Wood
Validation: Noemi Vergopolan
Visualization: Noemi Vergopolan
Writing – original draft: Noemi Vergopolan, Hylke E. Beck, Craig R.

1. Introduction

Soil moisture (SM) plays a key role in modulating water, energy, and carbon interactions between the land and atmosphere. As such, detailed information is essential for water resources management, natural hazards risk assessment, and understanding ecosystem dynamics, among others. However, SM varies strongly in space, with characteristic length scales ranging from a few centimeters to several kilometers depending on the landscape. SM hotspots that emerge from this spatial variability have significant implications for the scientific understanding and prediction of many hydrological and biogeochemical processes and applications. For instance, SM hotspots influence freshwater sources and agricultural management, as wet and dry conditions require different irrigation and fertilizer interventions for optimal crop growth (Franz et al., 2020; Sadri et al., 2020; Vergopolan et al., 2021). SM spatial variability leads to changes in surface temperature and evapotranspiration (Rouholahnejad Freund

Ferguson, Laura Torres-Rojas, Felix Eigenbrod, Wade Crow, Eric F. Wood
Writing – review & editing: Noemi Vergopolan, Justin Sheffield, Nathaniel W. Chaney, Ming Pan, Hylke E. Beck, Craig R. Ferguson

et al., 2020), altering drought impacts (Vergopolan et al., 2021) as well as the formation of clouds and convective storms (Simon et al., 2021; Zheng et al., 2021). SM hotspots can alter runoff generation, resulting in faster and peakier flood events (Zhu et al., 2018), and trigger wildfires (Holden et al., 2019; Taufik et al., 2017) and landslides (Brocca et al., 2016; Wang et al., 2020). SM spatial variability influences the distribution of soil fauna and flora, by controlling its habitats, food sources, and dynamics (He et al., 2015; Mathys et al., 2014; Sylvain et al., 2014; Youngquist & Boone, 2014). Depending on landscape characteristics (i.e., soils, topography, and vegetation), such SM-driven processes and hazards can occur at local spatial scales (1–100 m). Capturing the SM variability at local scales is critical to further our understanding of these processes and improve our modeling and prediction capabilities.

To this end, in-situ SM observations provide detailed information. However, networks of sensors are costly to deploy and maintain and, therefore, are not widely available over large areas. Microwave-based satellite measurements can provide global SM monitoring with 1–2 days revisit time (Chan et al., 2018; Gruber et al., 2019; Kerr et al., 2012), but retrievals are too coarse (9–36 km) to capture local-scale SM hotspots. Consequently, our current understanding of how SM varies locally is drawn primarily from site-specific studies using in-situ observations (Brocca et al., 2007, 2012; Choi & Jacobs, 2010; Crow et al., 2005, 2012; Famiglietti et al., 2008), airborne remote sensing imagery (Famiglietti et al., 2008; Garnaud et al., 2017) and hydrological modeling (Crow et al., 2005; Garnaud et al., 2017), or at larger scales using coarse resolution hydrological modeling (Li & Rodell, 2013; Manfreda et al., 2007) or satellite sensors (Das & Mohanty, 2006; Rötzer et al., 2015). These studies have provided a foundational understanding of how hydroclimate and landscape characteristics contribute to SM spatial variability and its underlining mechanisms (Vereecken et al., 2014). They characterize how SM spatial variability is impacted by precipitation (acting as a large-scale driver of runoff (Rosenbaum et al., 2012; Sivapalan et al., 1987)), topography (driving surface and subsurface water flow to the riparian zones (Famiglietti et al., 2008)), soil properties (controlling soil water storage, hydraulic conductivity, infiltration, and drying rates (Choi et al., 2007; Crow et al., 2012)), and vegetation (with time-varying physiological functioning influencing soil-water retention, infiltration, and evapotranspiration rates (Joshi & Mohanty, 2010; Mohanty et al., 2000)). However, SM interacts non-linearly with each of these hydroclimate and landscape drivers and as a result the impact of their combined interactions is complex (Vereecken et al., 2014). Because previous local-scale studies tend to be site-specific and with different experiment designs, the transferability of SM spatial variability across different hydroclimate and diverse landscapes is *unknown*. Consequently, there is no consensus on how the SM spatial variability plays out across different hydroclimates and landscapes, and how it influences water, energy, and carbon processes locally. Furthermore, little is known about how this variability persists across spatial scales, and whether it can be captured at regional scale by, for example, physical models and microwave satellite observations.

Here, we present the first characterization of local-scale SM spatial variability at a continental extent and we quantify the persistence of this variability across spatial scales. This assessment was enabled by SMAP-HydroBlocks – a newly developed 30-m satellite-based surface SM data set for the conterminous United States (CONUS) (Vergopolan et al., 2021a). SMAP-HydroBlocks' detailed and accurate SM estimates leverage recent scientific advances in the availability of data from in-situ SM networks, microwave-based satellite remote sensing, gridded meteorological datasets, high-resolution landscape physiography data, and hyper-resolution land surface modeling. As such, SMAP-HydroBlocks provides a unique tool to investigate the SM variability across scales and landscapes, and therefore can help elucidate the role of SM on water, energy, and carbon processes at spatial scales that have so far been unresolved (Blöschl et al., 2019). Toward this aim, this work (a) maps the magnitude of SM spatial variability across the CONUS, (b) quantifies the drivers and relationship with hydroclimate and landscape characteristics, and (c) reveals the multi-scale properties and persistence of this spatial variability across spatial scales. The SM spatial variability is striking in its complexity. We discuss the implications of this newly resolved SM variability for quantifying and understanding land-atmosphere interactions and applications in water resources, natural hazard risks, and ecosystem dynamics.

2. The Spatial Distribution of 30-m Soil Moisture Across the United States

SMAP-HydroBlocks (Vergopolan et al., 2021a) is the first hyper-resolution satellite-based surface SM product at a 30-m resolution over the conterminous United States (2015–2019). It uses a scalable cluster-based merging scheme (Vergopolan et al., 2020) which combines microwave satellite remote sensing, high-resolution land

surface model, radiative transfer modeling, machine learning, and in-situ observations to obtain hydrologically consistent SM estimates of the top 5-cm of the soil. SMAP-HydroBlocks was built upon NASA's Soil Moisture Active Passive L3 Enhanced Global 9-km satellite product (Chan et al., 2018; O'Neill et al., 2019) (SMAP L3E) and HydroBlocks, a field-scale resolving land surface model (Chaney et al., 2021). Validation using independent in-situ observations demonstrated its temporal and spatial representativeness and accuracy, particularly in capturing spatial extremes (Vergopolan et al., 2021a). SMAP-HydroBlocks details are available at Section S1 in Supporting Information S1.

The SM heterogeneity is demonstrated by SMAP-HydroBlocks substantial spatial variability from local to continental scales (Figure 1). At the continental scale, the SM variability reflects the SM interactions with large-scale hydroclimate and topographic features, with distinct drier conditions over the West and Southwest and wetter conditions over the Midwest, Corn Belt, Mississippi River basin, and Northeast. At the regional and local scales (Figure 1 insets), SMAP-HydroBlocks reveals detailed variations that emerge from the interactions between hydroclimate, topography, soil properties, and land use heterogeneity across the landscape. In the White River basin and the Appalachian Mountains, for example, we observe the imprint of small tributaries and wet riparian corridors in valleys and wetter conditions over vegetated lowlands. In the Mississippi floodplain the topography, historical meandric dunes, and agricultural fields modulate the SM spatial patterns. Over northern California in the Sierra Nevada, the riparian zone contrasts with the dry climate and local aridity.

3. What Is and What Drives the Spatial Variability in Soil Moisture?

The SM spatial variability across the CONUS is diverse. Here, we quantified using the spatial standard deviation (σ) – which measures the deviation of local wet and dry SM hotspots from spatial average conditions over a given domain. We calculated $\sigma_{30\ m}$ using the SMAP-HydroBlocks 30-m SM climatology (2015–2019) at each 10-km box across the CONUS (details in Section S2 in the Supporting Information S1). Results in Figure 2a show the largest SM spatial variability in the US Southern Coastal Plain, the lower Mississippi River, and the Great Lakes region, followed by moderate variability in the Northwestern Pacific, the Appalachian Mountains, and the Northeastern US. The magnitude of this variability is in agreement with the in-situ observational studies (Famiglietti et al., 2008; Vergopolan et al., 2020). Regions of high SM variability (shown in orange to red) are linked to wet locations with substantial precipitation, shallow water table depth (with abundant streams, ponds, wetlands), variable soil characteristics and verdant vegetation, which can exhibit significant contrast with respect to their surrounding environment. Low spatial variability is seen in most of the US Southwest (typically dry), and at the Northern of the US Great Plains and the Corn Belt, likely due to flat terrain and cropland dominance that reduces $\sigma_{30\ m}$.

To disentangle the relationships between SM spatial variability with the landscape and hydroclimate characteristics at each location, we performed a Principal Component Analysis (PCA) to identify associations with the magnitude of local wet and dry SM hotspots. In this context, the PCA is particularly useful because it indicates the data dominant modes of variation (i.e., the principal components) and quantifies how different physical characteristics co-vary, thus being particularly helpful for identifying strong patterns in big data. Here, in specific, the PCA compared the SM spatial standard deviation ($\sigma_{30\ m}$, Figure 2a) with the spatial mean (μ) and spatial standard deviation (σ) of high-resolution variables that modulate SM dynamics, such as soil properties (sand, clay, and silt content), vegetation greenness (e.g., the Normalized Difference Vegetation Index) and land cover types, elevation and topographic wetness, and climatologies of air temperature and precipitation at the same 10-km box. Section S3 in Supporting Information S1 details the PCA, the characteristics of these physical drivers, and their spatial distribution (Figures S1–S5 in Supporting Information S1).

SM variability tend to follow the dry to wet precipitation gradients (Figure 2a, Figure S5 in Supporting Information S1), this pattern is also evident in the PCA (Figure 2b). Results shows how the SM spatial variability (points) follows the first principal component (PC1), which is dominated by the precipitation (μ_{precip}) at locations with wetlands and shallow water table depths ($\mu_{wetland}$), the spatial variability in soil texture (σ_{clay}, σ_{sand}), mean and variability in the topographic wetness index (μ_{TWI}, σ_{TWI}) while the second component (PC2) is dominated by the soil texture content (μ_{clay}, μ_{sand}, μ_{silt}). In the West coast and most of the East US, precipitation drives SM spatial variability through the generation of runoff that is distributed differently across heterogeneous landscapes (Sivapalan et al., 1987) and, along with the warm temperatures in the South, influences in the long-term the

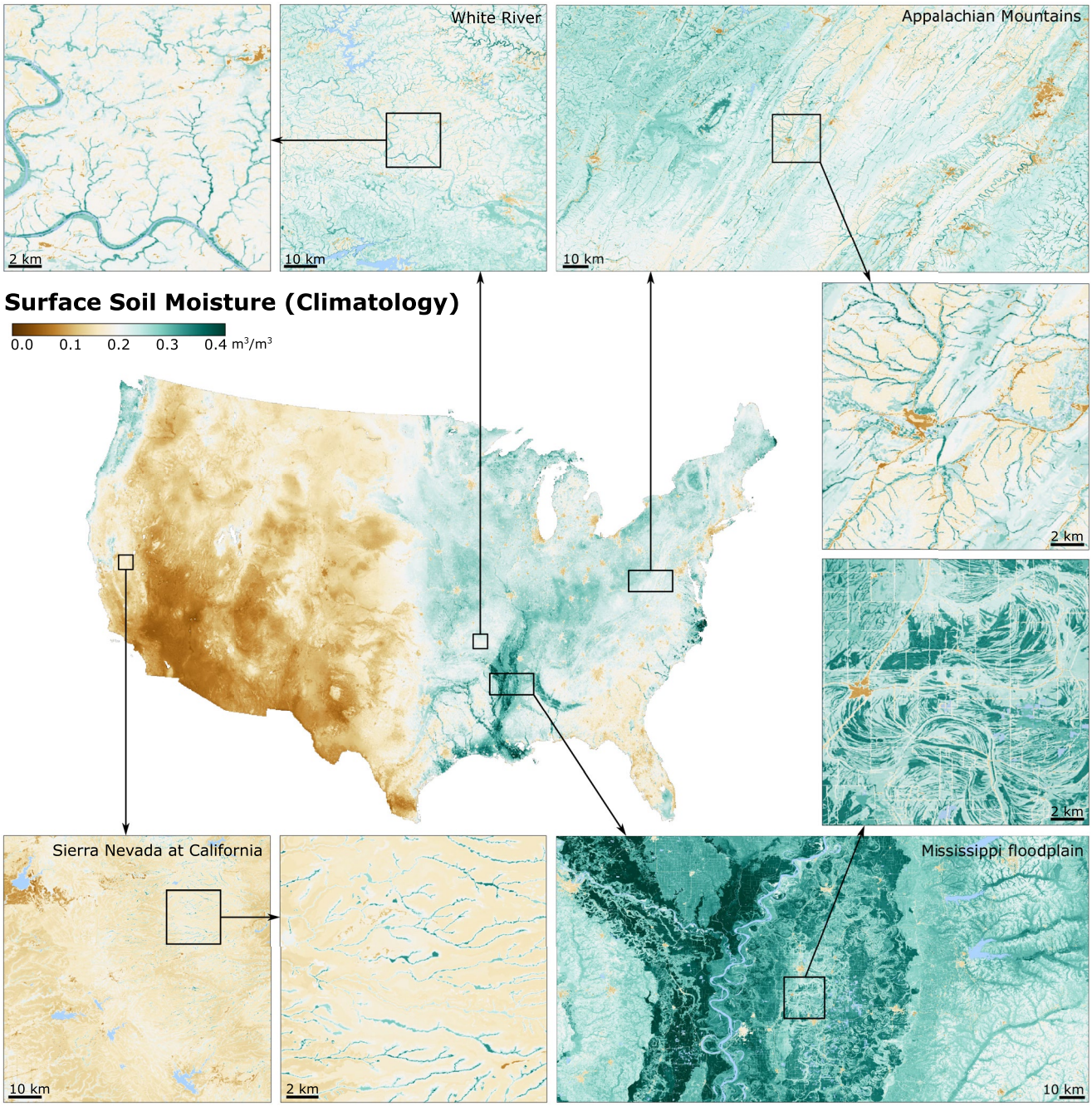

Figure 1. The spatial distribution of surface soil moisture climatology across the CONUS, as shown by the SMAP-HydroBlocks data set at 30-m spatial resolution (2015–2019). Insets highlight the spatial detail for selected locations with different hydroclimatic and topographical conditions. Water bodies are shown in blue, scale bar is shown at each panel. Interactive visualization of the 30-m data is available at https://waterai.earth/smaphb.

formation of topographic landscapes and soils through climate and chemical weathering (Breemen et al., 2002). Soil spatial heterogeneity and variations in its characteristics (e.g., texture, organic matter content, porosity, and structure) are largely observed in the US southeast and near the US Great lakes, and drive local variations in soil drying rates, hydraulic conductivity, and lateral water distribution (Choi et al., 2007; Crow et al., 2012), which in turn generates more spatially variable SM content. This spatial heterogeneity in soils (Figure S1 in Supporting Information S1) plays a particular role the SM variability in places with shallow water table depth, such as the US Southeast, lower and upper Mississippi River valleys (Figure 1a). Vegetation characteristics (e.g., type, density, and uniformity) and their changes in time (i.e., seasonal growth and decay) can dynamically influence

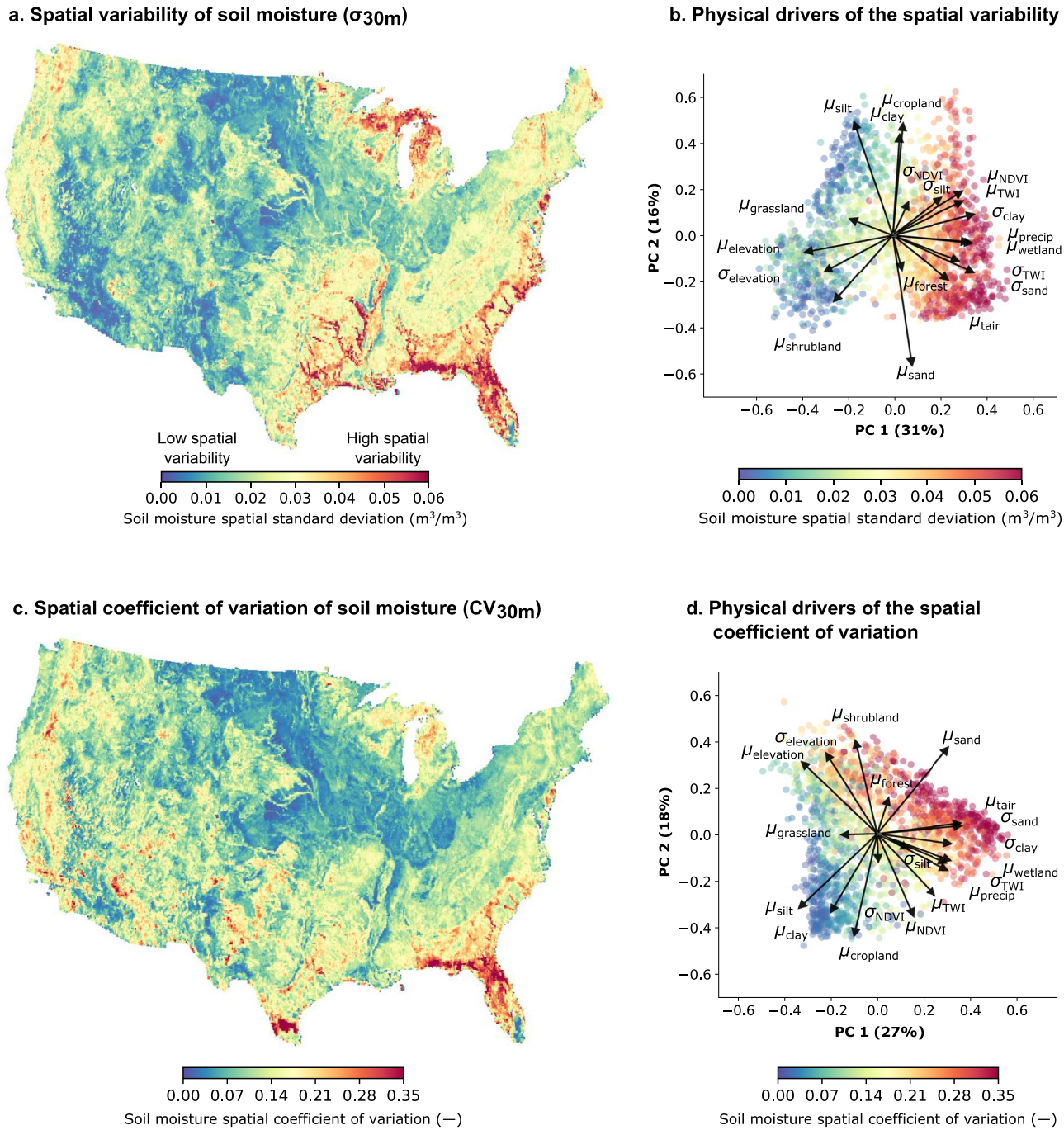

Figure 2. The spatial variability of local-scale soil moisture and its relationship with physical drivers. (a) As a proxy for soil moisture spatial variability, we calculated the spatial standard deviation of the 30-m resolution SMAP-HydroBlocks climatological SM (2015–2019) at each 10-km box across CONUS. Locations in red show where soil moisture spatial variability is highest. (b) The PCA biplot compares the first two components of the relationship between the spatial standard deviation of the 30-m SM (points) with physical characteristics' spatial mean (μ) and spatial standard deviation (σ) within the same 10-km box (arrows). Similarly, (c) shows the map of the spatial coefficient of variation of SM (as the ratio between spatial standard deviation and the spatial mean), also calculated at each 10-km box, and (d) shows the correspondent Principal Component Analysis (PCA) biplot. Figures S1–S5 in Supporting Information S1 shows the spatial variation of the physical drivers. In the PCA biplots, each arrow represents the loading of a physical driver and its direction of variation represents how strongly each driver influences a principal component. The angles between the arrows indicate how the physical characteristics correlate with one another. Arrows pointing toward red (blue) dots show the drivers' direction of high (low) SM spatial variability.

SM variability as its physiological functioning and distribution and density of roots can affect soil-water retention, infiltration, and evapotranspiration rates (Mohanty et al., 2000). Results show high vegetation greenness (μ_{NDVI}) and its spatial variability (σ_{NDVI}), correspond to wet locations of high SM spatial variability (e.g., at the East and West coast). In contrast, in the West the dry conditions and dominant $\mu_{shrubland}$ and $\mu_{grassland}$ types leads to lower SM spatial variability.

Topographic characteristics (e.g., surface elevation, slope, topographic wetness index, aspect, and curvature) drive SM convergence to riparian zones via surface and subsurface lateral flow (Crow et al., 2012). Results show high SM variability linked to high topographic wetness index (μ_{TWI}) and its spatial variability (σ_{TWI}), demonstrating the role of topography in driving SM spatial patterns, particularly at the US Southeast coast, lower and upper Mississippi basins. However, topographic control on surface SM tends to happen mostly during and after rainfall events (Western et al., 2003). In contrast, during drydown and typical conditions, the influence of soil properties and vegetation will dominate (Chang & Islam, 2003; Ryu & Famiglietti, 2005). In fact, the results also show locations of high elevation ($\mu_{elevation}$) and spatially variable topography ($\sigma_{elevation}$), as in most of the US West, linked to low SM spatial variability (Figure 2b) because most of the locations of high elevation gradients in the West tend to be climatologically drier (Figure S6 in Supporting Information S1). In contrast, at climatologically wet locations, such as over the Appalachian mountains (Figures 1 and 2a), substantial SM spatial variability is shown. SM spatial variability is known to be higher at wetter soils (Famiglietti et al., 2008). To isolate the contribution of other physical drivers from the influence of dry/wet conditions, we computed the SM spatial coefficient of variation ($CV_{30\ m}$), which represents the SM spatial variability normalized by the soil wetness (Figure 2c). The PCA of $CV_{30\ m}$ (Figure 2d) shows that spatial variability in soil texture (σ_{clay}, σ_{sand}) still dominates with the SM variability, followed by air temperature (μ_{tair}) and sand content (μ_{sand}). This is particularly evident over the US Southeast where high spatially variable and quick drying sandy soils at the surface interact with low water table depths and wetlands and results in distinct wet and dry SM hotpots. Figure 2d also shows the topographic drivers ($\mu_{elevation}$, $\sigma_{elevation}$, μ_{TWI}, and σ_{TWI}), vegetation characteristics (μ_{NDVI}, σ_{NDVI}, $\mu_{shrubland}$, μ_{forest}), and precipitation (μ_{precip}) shifted toward PC2, highlighting their secondary role in driving the SM $CV_{30\ m}$. As shown here, the strength of SM hotspots and their local spatial variability emerges from the combined and non-linear hydrological processes and their interactions with climatic conditions, topography, soils, and vegetation dynamics. However, at each location, different characteristics and physical processes will contribute differently and lead to patterns that cannot be generalized by the independent contribution of a few key drivers.

4. Where and How Does Soil Moisture Variability Persists Across Spatial Scales?

Depending on the landscape complexity, the SM spatial variability at the local scale may not persist at regional scales and therefore cannot be represented by coarse resolution data (e.g., from models or microwave satellite observations). The inability to represent this variability dampens the strength of local SM hotspots and could hamper the utility of SM information for water resources management and understanding of land-atmosphere interactions at local scales. In fact, quantifying how SM spatial variability changes across scales and its impact on the Earth system remains a critical unsolved problem in hydrology (Blöschl et al., 2019; Crow et al., 2012). Here, we characterize the scaling properties of SM spatial variability by mapping how this variability changes across spatial scales and where it persists. This also helps to identify where high-resolution data is critical to capture local-scale variability.

To this end, we performed a synthetic spatial scaling analysis, which involves upscaling the 30-m SMAP-HydroBlocks data to coarser spatial scales (λ_{scale}: 60 m, 90 m, …, 1 km) and calculating the change in spatial standard deviation (i.e., change in variability) at each scale with respect to the 30-m data ($\sigma_{scale}/\sigma_{30\ m}$). Observational studies at a few sites have shown that this change in SM spatial variability with data supporting scale and spacing follows a power-law relationship (Rodriguez-Iturbe et al., 1995). This behavior turned out to be the same observed when comparing SM correlation length and distance, and it often characterizes complex hydrological fractal nature (Famiglietti et al., 2008). As illustrated in Figure 3, the log relationship between the spatial standard deviation ratio and data scale indicates the strength of the SM spatial scale dependency through β, and it can be interpreted as an indicator of SM variability persistence across scales (Hu et al., 1997). The more negative the β, the larger is the dependency of the SM spatial variability on the data scale. Consequently, higher information loss (herein defined as $1 - \sigma_{scale}/\sigma_{30\ m}$) and lower variability persistence are expected at coarser spatial resolutions. Although SM spatial patterns can change over time, its spatial signature persists

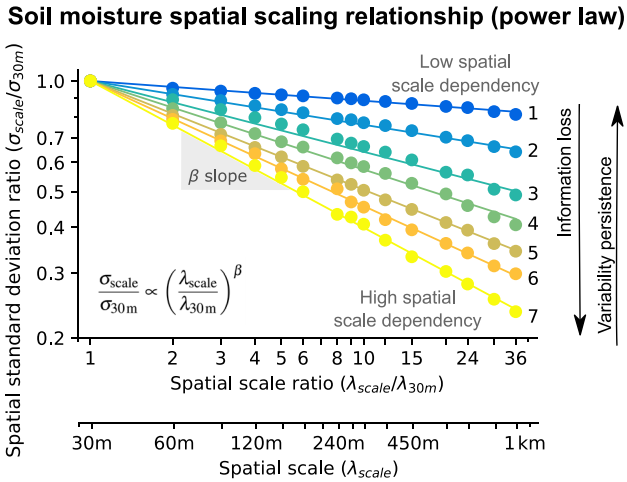

Figure 3. The scaling of soil moisture spatial variability. Illustration shows how soil spatial scaling follows a power-law relationship. The graph compares the soil moisture spatial standard deviation ratio of data at a coarse spatial scale with respect to the 30-m data ($\sigma_{scale}/\sigma_{30\,m}$). As the spatial scale increases (decreasing spatial resolution), the spatial standard deviation ratio decreases. The decrease in spatial variability follows a power-law relationship. β quantifies the strength of the inverse relationship between data scale and spatial variability. The larger the β slope, the larger is the spatial-scale dependency, meaning that the SM spatial variability does not persist and there is a larger information loss at coarser spatial scales. We selected seven locations across the CONUS (shown in Figure 4b) that illustrate a range of different scaling behaviors (lines).

(Mälicke et al., 2020). As a result, β does not change significantly over time (e.g., during SM drydown) making it a stable metric for characterizing multi-scaling SM properties (Oldak et al., 2002).

The scaling relationship for selected sites of varying landscape complexity are illustrate in Figures 3 and 4a. The small β value of −0.06 (Location 1, Figure 3) indicates little change in spatial standard deviation with scale and persistence of local-scale SM hotspots across scales. At 1-km resolution, only 21% of the spatial variability is lost with respect to the 30-m data (Figure 4a, first row). In contrast, the scaling relationship at Location 7 shows a large β (−0.37) associated with a 74% reduction in spatial variability. In fact, the imprint of the riparian zone within this site vanishes at 1-km resolution (Figure 4a last row), exemplifying the high spatial scale dependency and lack of spatial variability persistence. Figure 4b maps the information loss (as a percentage) when the 30-m SM data is averaged to 1-km resolution (Figure S7 in Supporting Information S1 maps the β coefficient) across CONUS. Overall, there is little persistence of SM spatial variability across scales, with an average information loss of 48 ± 10%, and a maximum loss of 80%. Importantly, this information loss (and the associated β) strongly varies by location, revealing complex context-dependent multi-scale properties (Figure 4b). A PCA in Figure 4d compares the strength of this information loss with the mean and spatial variability of landscape and climate characteristics. Results showed a tendency for high information loss at locations with strong topographic gradients (such as over the Rocky Mountains, Appalachian Mountains, Northwestern Cascade Range, and the Sierra Nevada) and dominant forest coverage (e.g., most of the Northeast). However, for information loss below 60% the results shows no clear or generalizable relationship with climatic and physiographic characteristics. We also compared the relationship between information loss and SM spatial standard deviation (Figure 5a). High and low information loss can emerge from either high or low SM spatial variability, but with zero correlation. This demonstrates how the complex and non-linear hydrological, ecohydrological, and biogeochemical processes that occur at local scales yield such unique SM scaling behavior locally that can hardly be transferred to different hydroclimates and landscapes.

Mapping where SM spatial variability and information loss are highest is critical to identify where high-resolution data is needed. Figure 5b shows low SM spatial variability with high information loss (dark blue) in most of the US Corn Belt and the Missouri River basin, driven mainly by cropland dominance and flat terrain. These small-scale variations vanish at the 1-km resolution but are critical to capturing intra-field scale irrigation water demands (Franz et al., 2020). Low variability with high information loss is also observed in parts of the Rocky Mountains and the West, where dry conditions lead to low SM variability. However, topographic gradients enhance information loss, hampering the monitoring of (already scarce) freshwater resources. High SM variability and information loss (dark orange) are present on the US West coast (e.g., Sierras Nevada and the Cascade Range) and most of the Northeastern US (including the Appalachians), driven by precipitation interactions with topography that replenishes the riparian zones. High SM variability and information loss are also evident near the US Great Lakes, lower Mississippi River, and the Southeast coast, driven by heterogeneity in soils driving spatially variable SM dry-down rates contrasting with wetlands and shallow water table depths. Given the high SM variability and information loss, further allocating in-situ monitoring resources at these locations is thus critical for better monitoring and quantifying non-linear SM-dependent hydrological, ecological, and biogeochemical processes.

5. Implications

5.1. Understanding and Modeling Land-Atmosphere Feedbacks

Studies have shown how neglecting the SM spatial variability at local scales dampens extremes and introduces errors when quantifying scale-dependent water, energy, and carbon interactions between the land and the atmosphere. For example, the relationship between SM and evapotranspiration under different water and energy

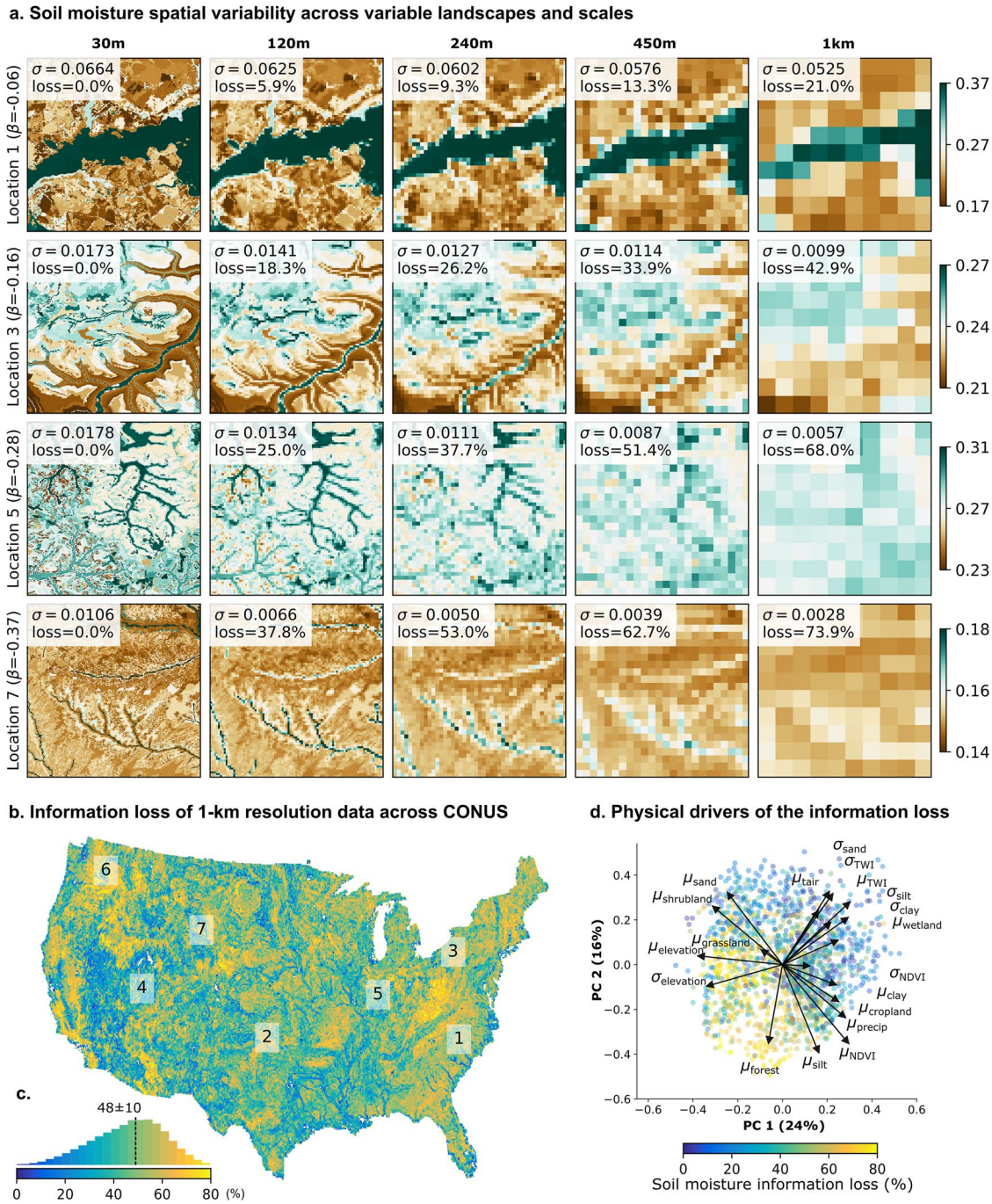

Figure 4. The information loss of soil moisture across spatial scales. (a) Comparison of the soil moisture data at different spatial resolutions: each panel shows SM at a 10-km box with its climatological spatial variability (measured by the spatial standard deviation, σ), and information loss (measured as the percentage change in spatial standard deviation with respect to the 30-m data). Each row shows a different location (subsetted from the 7 locations in Figure 3) and each column shows data at different resolutions. (b) We mapped the information loss of the 1-km resolution data for each 10-km box across the CONUS. Locations in orange to yellow show where coarser spatial resolution data fail to capture 60%–80% of the spatial variability observed at 30-m resolution. Subplot (c) shows the distribution of this information loss in the US. (d) PCA biplot compares the first two components of the relationship between the information loss (points) with physical characteristics' spatial mean (μ) and spatial standard deviation (σ) within the same 10-km boxes (arrows). Figures S1–S5 in Supporting Information S1 shows the spatial variation of the physical drivers. Each arrow represents the loading of a physical driver and its direction of variation represents how strongly each driver influences a principal component. The angles between the arrows indicate how the physical characteristics correlate with one another. Arrows pointing toward yellow (blue) dots show the drivers' direction of high (low) soil moisture information loss.

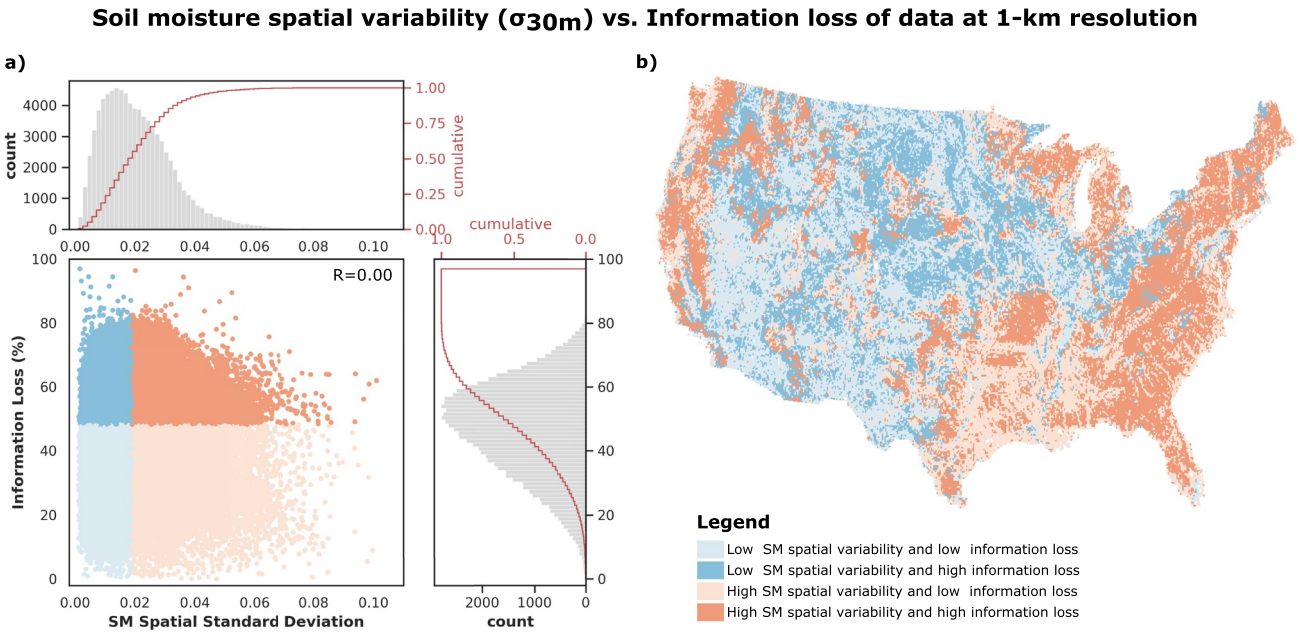

Figure 5. Comparison between the spatial variability of SM data at 30-m resolution and information loss of the 1-km resolution SM data. Panel (a) compares the joint distribution of the SM spatial standard deviation (*x*-axis) and the information loss (*y*-axis) of all 10-km boxes across CONUS. To identify locations with low or high SM spatial variability and information loss, the data space was partitioned in 4 domains, based on the average SM spatial standard deviation (0.02) and average information loss (48%). Adjacent top and lateral graphs show the histograms and cumulative functions of the SM spatial standard deviation and information loss, respectively. Panel (b) maps each of the 4 domains with the same color scheme: blue (orange) colors show areas of low (high) SM spatial variability, whereas light (dark) colors show areas of low (high) information loss. In panel b, orange colors emphasize the high SM variability patterns (observed in Figure 2a), while the dark (blue and orange) colors emphasize the high information loss patterns (observed in Figure 4b).

constraints is highly non-linear (Rouholahnejad Freund & Kirchner, 2017). When wet SM hotspots are resolved at spatial scales closer to their true spatial variability, they enhance evapotranspiration to the atmosphere in comparison to spatially homogeneous drier conditions (Crow & Wood, 2002; Rouholahnejad Freund et al., 2020). This higher evapotranspiration further cools the ground surface, and can enhance horizontal atmospheric humidity and temperature gradients that drive variable boundary layer dynamics, development of large-scale eddies, potentially triggering of local convective rainfall (Ford et al., 2015; Simon et al., 2021; Vergopolan & Fisher, 2016; Zheng et al., 2021). Spatially variable SM also controls plant photosynthesis rates and nutrient cycling, yielding non-linear changes of 40%–80% in carbon uptake (Green et al., 2019; Trugman et al., 2018) and 78% nitrogen cycling (Paul et al., 2003). For instance, optimal crop nitrogen uptake is inhibited by both very dry and wet SM conditions. While dry SM inhibits mineralization, extreme wet SM lead to denitrification and N_2O release (Paul et al., 2003) — a greenhouse gas 298 times more effective at trapping heat in the atmosphere than CO_2 (Denman et al., 2007). As such, the spatial variability in SM critically changes the flux response of highly non-linear and local-scale processes, while grid-average conditions can lead to inaccurate assessment and process interpretation. Limited observations have historically constrained understanding of the impact of SM variability on these processes. The spatial variability of SMAP-HydroBlocks allows quantifying these processes' dependencies and identifying where fine-scale data is critical for improving our understanding of the land-atmosphere and biogeochemical processes that drive changes in weather and climate and our ability to model them.

5.2. Supporting Water Resources Decision-Making and Natural Hazards Risks

Local scale SM spatial variability also impacts management of freshwater resources and water-dependent risks. For instance, when local dry or wet SM hotspots are averaged by coarse-resolution SM data, the perceived intensity of drought conditions or extent of waterlogging is reduced. The related underestimation (or overestimation) of crop water demands limits farmer decision making on when and where to irrigate (Franz et al., 2020; Vergopolan et al., 2021). Capturing SM dynamics at the field scale is thus critical to quantify irrigation (Dari et al., 2020; Jalilvand et al., 2019). SM spatial variability also impacts on wildfires by controlling the spatial

distribution of vegetation fuel load and flammability through vegetation water content (O et al., 2020; Taufik et al., 2017). As such, the inability to represent wet and dry SM hotspots at sub-kilometer scales results in underestimated risks of propagating wildfires (Holden et al., 2019). Similarly, local wet hotspots lead to conditions that trigger landslides and local flash floods. Landslides tends to happen at small-scale (e.g., ∼10–100-m^2, Zhang et al. (2019)) and occur when soil water saturation increases soil-column weight, reduces soil cohesion, and leads to gravity-driven mass movements. Wet hotspots that trigger these events are mostly averaged out by coarser-resolution data, critically limiting monitoring of slope stability and landslide detection accuracy (Wang et al., 2020). Spatially variable SM also drives spatial variability rainfall infiltration rates which influence the timing and spatial structure of runoff generation and flooding, leading to earlier and more intense floods (Zhu et al., 2018).

5.3. Monitoring and Understanding Biodiversity and Species Distribution

SM spatial variability plays a critical role in controlling land ecosystems (Rodríguez-Iturbe & Porporato, 2007), particularly soil organisms and communities (Mathys et al., 2014; Sylvain et al., 2014), but also amphibian movements (Youngquist & Boone, 2014), and species distributions more generally (Gardner et al., 2019). Soil organisms that are closely coupled with SM are especially important as they comprise 25%–33% of Earth's biodiversity (Decaëns et al., 2006), providing vital ecosystem functions such as soil fertilization, nutrient recycling, pest and disease regulation, and erosion control (Qiu & Turner, 2015; Wall, 2013). Variability in SM leads to patchy and reduced distribution of suitable habitats for such soil organisms and influence their dynamics (Wall & Virginia, 1999). Particularly in arid and degraded conditions, this leads to reduced local biodiversity and ecosystem function and to increased susceptibility to disturbances (Wall & Virginia, 1999). Therefore, characterization of SM spatial variability and information loss provide insights on organisms' dynamics, behavior, biodiversity richness, and ecosystem service provision (He et al., 2015). SM also plays a critical role in determining the degree of drought stress of plants (Vergopolan et al., 2021); a failure to account for local variability can lead to underestimates of the effects of climate change on future distributions (Midgley et al., 2002). In addition, SM play a key role in enabling detailed monitoring of pest infestation food sources and reproduction pathways (Gómez et al., 2020), and supporting the assessment and forecasting of infectious disease and pest risks such as West Nile virus, malaria, and locust swarms (Escorihuela et al., 2018; Keyel et al., 2019). Understanding SM variability and scaling at the local scale is therefore critical for improving understanding and monitoring of ecosystems dynamics, pest infestations, and biodiversity loss in a spatially explicit manner. Furthermore, it supports the development of adaptation pathways toward improving these ecosystems' resilience to climate variability and climate change.

6. Conclusion

Understanding SM spatial variability, its scaling behavior, and effects on freshwater resources is a long-standing grand challenge in hydrology. By mapping SM variability at unprecedented scales, our study reveals the unseen and striking local-scale variability across CONUS. The magnitude of this variability and information loss across scales varies widely across landscapes, highlighting how SM-dependent water, energy, and carbon processes cannot be reduced to simplistic relations with hydroclimate or landscape characteristics. Yet, this local-scale complexity demonstrated by SMAP-HydroBlocks is not represented by current SM monitoring and modeling systems (1–25-km resolution) and hinders our ability to address a range of scientific questions and applications on land-atmosphere feedbacks, water resources management, and biodiversity and species distributions. The SM variability and information loss mapped here can critically aid resources allocation and design of in-situ networks for improved monitoring of non-linear and SM-dependent hydrological, biogeochemical and ecological processes. Given recent advances in data availability and computing resources, the next generation of SM products, land surface models, and Earth system models should also consider how to account for this local scale variability to more realistically represent hydrological processes, natural hazards, and its interactions with climate. By mapping the SM variability and its scaling behavior, this work provides a pathway toward improving the understanding and quantification of hydrological, biogeochemical, and ecological processes at spatial scales that have so far been unresolved.

Data Availability Statement

The SMAP-HydroBlocks surface soil moisture data set at 30-m 6-h resolution (2015–2019) comprises a 62 TB data set (with maximum compression). Due to the storage limitation of online repositories, we provide the raw data at the Hydrologic Response Unit (HRU) level (time, hru) compressed to 33 GB. Python code and instructions for post-processing the data into geographic coordinates (time, latitude, longitude) is available at GitHub (https://github.com/NoemiVergopolan/SMAP-HydroBlocks_postprocessing). Data are available for download at Vergopolan et al. (2021b) (https://doi.org/10.5281/zenodo.5206725). The data are provided in netCDF-4 format (https://www.unidata.ucar.edu/software/netcdf/), and referenced to the World Geodetic Reference System 1984 (WGS 84) ellipsoid. The netCDF-4 files can be viewed, edited, and analyzed using most Geographic Information Systems (GIS) software packages, including ArcGIS, QGIS, and GRASS. As an illustration example, a 30-m map of the SMAP-HydroBlocks annual and long-term climatology can be viewed through an interactive web interface at https://waterai.earth/smaphb.

Acknowledgments
This work was supported by the "Modernizing Observation Operator and Error Assessment for Assimilating In-situ and Remotely Sensed Snow/Soil Moisture Measurements into NWM" project from NOAA (grant number NA19OAR4590199), the "Understanding Changes in High Mountain Asia project" project from NASA (grant number NNH19ZDA001N-HMA), the NASA-NOAA Interagency Agreement through the High Mountain Asia program (grant number 80HQTR21T0015), the "A new paradigm in precision agriculture: assimilation of ultra-fine resolution data into a crop-yield forecasting model" project from the King Abdullah University of Science and Technology (grant number OSR-2017-CRG6), and the "Building REsearch Capacity for sustainable water and food security In drylands of sub-saharan Africa (BREC-cIA)" project from the UK Research and Innovation as part of the Global Challenges Research Fund (grant number NE/P021093/1).

References

Blöschl, G., Bierkens, M. F., Chambel, A., Cudennec, C., Destouni, G., Fiori, A., et al. (2019). Twenty-three unsolved problems in hydrology (UPH) – A community perspective. *Hydrological Sciences Journal*, *64*(10), 1–18. https://doi.org/10.1080/02626667.2019.1620507

Breemen, N. V., Buurman, P., & Ebrary, I. (2002). *Soil formation*. Kluwer Academic.

Brocca, L., Ciabatta, L., Moramarco, T., Ponziani, F., Berni, N., & Wagner, W. (2016). Use of satellite soil moisture products for the operational mitigation of landslides risk in central Italy. *Satellite Soil Moisture Retrieval*, 231–247. https://doi.org/10.1016/b978-0-12-803388-3.00012-7

Brocca, L., Morbidelli, R., Melone, F., & Moramarco, T. (2007). Soil moisture spatial variability in experimental areas of central Italy. *Journal of Hydrology*, *333*(2–4), 356–373. https://doi.org/10.1016/j.jhydrol.2006.09.004

Brocca, L., Tullo, T., Melone, F., Moramarco, T., & Morbidelli, R. (2012). Catchment scale soil moisture spatial–temporal variability. *Journal of Hydrology*, *422–423*, 63–75. https://doi.org/10.1016/j.jhydrol.2011.12.039

Chan, S., Bindlish, R., O'Neill, P., Jackson, T., Njoku, E., Dunbar, S., et al. (2018). Development and assessment of the SMAP enhanced passive soil moisture product. *Remote Sensing of Environment*, *204*, 931–941. https://doi.org/10.1016/j.rse.2017.08.025

Chaney, N. W., Torres-Rojas, L., Vergopolan, N., & Fisher, C. K. (2021). Hydroblocks v0.2: Enabling a field-scale two-way coupling between the land surface and river networks in Earth system models. *Geoscientific Model Development*, *14*(11), 6813–6832. https://doi.org/10.5194/gmd-14-6813-2021

Chang, D. H., & Islam, S. (2003). *Effects of topography, soil properties and mean soil moisture on the spatial distribution of soil moisture: A stochastic analysis*. (pp. 193–225). CRC Press.

Choi, M., & Jacobs, J. M. (2010). Spatial soil moisture scaling structure during soil moisture experiment 2005. *Hydrological Processes*, *25*(6), 926–932. https://doi.org/10.1002/hyp.7877

Choi, M., Jacobs, J. M., & Cosh, M. H. (2007). Scaled spatial variability of soil moisture fields. *Geophysical Research Letters*, *34*(1), L01401. https://doi.org/10.1029/2006gl028247

Crow, W. T., Berg, A. A., Cosh, M. H., Loew, A., Mohanty, B. P., Panciera, R., et al. (2012). Upscaling sparse ground-based soil moisture observations for the validation of coarse-resolution satellite soil moisture products. *Reviews of Geophysics*, *50*(2). https://doi.org/10.1029/2011rg000372

Crow, W. T., Ryu, D., & Famiglietti, J. S. (2005). Upscaling of field-scale soil moisture measurements using distributed land surface modeling. *Advances in Water Resources*, *28*, 1–14. https://doi.org/10.1016/j.advwatres.2004.10.004

Crow, W. T., & Wood, E. F. (2002). The value of coarse-scale soil moisture observations for regional surface energy balance modeling. *Journal of Hydrometeorology*, *3*(4), 467–482. https://doi.org/10.1175/1525-7541(2002)003<0467:tvocss>2.0.co;2

Dari, J., Brocca, L., Quintana-Seguí, P., Escorihuela, M. J., Stefan, V., & Morbidelli, R. (2020). Exploiting high-resolution remote sensing soil moisture to estimate irrigation water amounts over a mediterranean region. *Remote Sensing*, *12*(16), 2593. https://doi.org/10.3390/rs12162593

Das, N. N., & Mohanty, B. P. (2006). Root zone soil moisture assessment using remote sensing and vadose zone modeling. *Vadose Zone Journal*, *5*(1), 296–307. https://doi.org/10.2136/vzj2005.0033

Decaëns, T., Jiménez, J., Gioia, C., Measey, G., & Lavelle, P. (2006). The values of soil animals for conservation biology. *European Journal of Soil Biology*, *42*, S23–S38. https://doi.org/10.1016/j.ejsobi.2006.07.001

Denman, K. L., Brasseur, G., Chidthaisong, A., Ciais, P., Cox, P. M., Dickinson, R. E., et al. (2007). *Couplings between changes in the climate system and biogeochemistry*. (pp. 499–588). Cambridge University Press.

Escorihuela, M. J., Merlin, O., Stefan, V., Moyano, G., Eweys, O. A., Zribi, M., et al. (2018). SMOS based high resolution soil moisture estimates for desert locust preventive management. *Remote Sensing Applications: Society and Environment*, *11*, 140–150. https://doi.org/10.1016/j.rsase.2018.06.002

Famiglietti, J. S., Ryu, D., Berg, A. A., Rodell, M., & Jackson, T. J. (2008). Field observations of soil moisture variability across scales. *Water Resources Research*, *44*(1). https://doi.org/10.1029/2006wr005804

Ford, T. W., Rapp, A. D., Quiring, S. M., & Blake, J. (2015). Soil moisture–precipitation coupling: Observations from the Oklahoma mesonet and underlying physical mechanisms. *Hydrology and Earth System Sciences*, *19*(8), 3617–3631. https://doi.org/10.5194/hess-19-3617-2015

Franz, T. E., Pokal, S., Gibson, J. P., Zhou, Y., Gholizadeh, H., Tenorio, F. A., et al. (2020). The role of topography, soil, and remotely sensed vegetation condition towards predicting crop yield. *Field Crops Research*, *252*, 107788. https://doi.org/10.1016/j.fcr.2020.107788

Gardner, A. S., Maclean, I. M., & Gaston, K. J. (2019). Climatic predictors of species distributions neglect biophysiologically meaningful variables. *Diversity and Distributions*, ddi.12939. https://doi.org/10.1111/ddi.12939

Garnaud, C., Bélair, S., Carrera, M. L., McNairn, H., & Pacheco, A. (2017). Field-scale spatial variability of soil moisture and l-band brightness temperature from land surface modeling. *Journal of Hydrometeorology*, *18*(3), 573–589. https://doi.org/10.1175/jhm-d-16-0131.1

Gómez, D., Salvador, P., Sanz, J., & Casanova, J. L. (2020). Modelling desert locust presences using 32-year soil moisture data on a large-scale. *Ecological Indicators*, *117*, 106655. https://doi.org/10.1016/j.ecolind.2020.106655

Green, J. K., Seneviratne, S. I., Berg, A. M., Findell, K. L., Hagemann, S., Lawrence, D. M., & Gentine, P. (2019). Large influence of soil moisture on long-term terrestrial carbon uptake. *Nature*, *565*(7740), 476–479. https://doi.org/10.1038/s41586-018-0848-x

Gruber, A., Scanlon, T., van der Schalie, R., Wagner, W., & Dorigo, W. (2019). Evolution of the ESA CCI soil moisture climate data records and their underlying merging methodology. *Earth System Science Data*, *11*(2), 717–739. https://doi.org/10.5194/essd-11-717-2019

He, K. S., Bradley, B. A., Cord, A. F., Rocchini, D., Tuanmu, M.-N., Schmidtlein, S., et al. (2015). Will remote sensing shape the next generation of species distribution models? *Remote Sensing in Ecology and Conservation*, *1*, 4–18. https://doi.org/10.1002/rse2.7

Holden, Z. A., Jolly, W. M., Swanson, A., Warren, D. A., Jencso, K., Maneta, M., et al. (2019). Topofire: A topographically resolved wildfire danger and drought monitoring system for the conterminous United States. *Bulletin of the American Meteorological Society*, *100*(9), 1607–1613. https://doi.org/10.1175/bams-d-18-0178.1

Hu, Z., Islam, S., & Cheng, Y. (1997). Statistical characterization of remotely sensed soil moisture images. *Remote Sensing of Environment*, *61*(2), 310–318. https://doi.org/10.1016/s0034-4257(97)89498-9

Jalilvand, E., Tajrishy, M., Ghazi Zadeh Hashemi, S. A., & Brocca, L. (2019). Quantification of irrigation water using remote sensing of soil moisture in a semi-arid region. *Remote Sensing of Environment*, *231*, 111226. https://doi.org/10.1016/j.rse.2019.111226

Joshi, C., & Mohanty, B. P. (2010). Physical controls of near-surface soil moisture across varying spatial scales in an agricultural landscape during SMEX02. *Water Resources Research*, *46*(12). https://doi.org/10.1029/2010wr009152

Kerr, Y. H., Waldteufel, P., Richaume, P., Wigneron, J. P., Ferrazzoli, P., Mahmoodi, A., et al. (2012). The SMOS soil moisture retrieval algorithm. *IEEE Transactions on Geoscience and Remote Sensing*, *50*(5), 1384–1403. https://doi.org/10.1109/tgrs.2012.2184548

Keyel, A. C., Elison Timm, O., Backenson, P. B., Prussing, C., Quinones, S., McDonough, K. A., et al. (2019). Seasonal temperatures and hydrological conditions improve the prediction of West Nile virus infection rates in Culex mosquitoes and human case counts in New York and Connecticut. *PLoS One*, *14*(6), e0217854. https://doi.org/10.1371/journal.pone.0217854

Li, B., & Rodell, M. (2013). Spatial variability and its scale dependency of observed and modeled soil moisture over different climate regions. *Hydrology and Earth System Sciences*, *17*(3), 1177–1188. https://doi.org/10.5194/hess-17-1177-2013

Mälicke, M., Hassler, S. K., Blume, T., Weiler, M., & Zehe, E. (2020). Soil moisture: Variable in space but redundant in time. *Hydrology and Earth System Sciences*, *24*(5), 2633–2653. https://doi.org/10.5194/hess-24-2633-2020

Manfreda, S., McCabe, M. F., Fiorentino, M., Rodríguez-Iturbe, I., & Wood, E. F. (2007). Scaling characteristics of spatial patterns of soil moisture from distributed modelling. *Advances in Water Resources*, *30*(10), 2145–2150. https://doi.org/10.1016/j.advwatres.2006.07.009

Mathys, A., Coops, N. C., & Waring, R. H. (2014). Soil water availability effects on the distribution of 20 tree species in Western North America. *Forest Ecology and Management*, *313*, 144–152. https://doi.org/10.1016/j.foreco.2013.11.005

Midgley, G., Hannah, L., Millar, D., Rutherford, M., & Powrie, L. (2002). Assessing the vulnerability of species richness to anthropogenic climate change in a biodiversity hotspot. *Global Ecology and Biogeography*, *11*(6), 445–451. https://doi.org/10.1046/j.1466-822x.2002.00307.x

Mohanty, B. P., Famiglietti, J. S., & Skaggs, T. H. (2000). Evolution of soil moisture spatial structure in a mixed vegetation pixel during the Southern Great Plains 1997 (SGP97) hydrology experiment. *Water Resources Research*, *36*(12), 3675–3686. https://doi.org/10.1029/2000wr900258

O, S., Hou, X., & Orth, R. (2020). Observational evidence of wildfire-promoting soil moisture anomalies. *Scientific Reports*, *10*(1), 11008. https://doi.org/10.1038/s41598-020-67530-4

O'Neill, P., Chan, S., Njoku, E. G., Jackson, T., Bindlish, R., & Chaubell, J. (2019). SMAP enhanced l3 radiometer global daily 9 km ease-grid soil moisture, version 3. https://doi.org/10.5067/T90W6VRLCBHI

Oldak, A., Pachepsky, Y., Jackson, T. J., & Rawls, W. J. (2002). Statistical properties of soil moisture images revisited. *Journal of Hydrology*, *255*(1–4), 12–24. https://doi.org/10.1016/s0022-1694(01)00507-8

Paul, K. I., Polglase, P. J., O'Connell, A. M., Carlyle, J. C., Smethurst, P. J., & Khanna, P. K. (2003). Defining the relation between soil water content and net nitrogen mineralization. *European Journal of Soil Science*, *54*(1), 39–48. https://doi.org/10.1046/j.1365-2389.2003.00502.x

Qiu, J., & Turner, M. G. (2015). Importance of landscape heterogeneity in sustaining hydrologic ecosystem services in an agricultural watershed. *Ecosphere*, *6*(11), art229. https://doi.org/10.1890/es15-00312.1

Rodríguez-Iturbe, I., & Porporato, A. (2007). *Ecohydrology of water-controlled ecosystems: Soil moisture and plant dynamics*. Cambridge University Press.

Rodriguez-Iturbe, I., Vogel, G. K., Rigon, R., Entekhabi, D., Castelli, F., & Rinaldo, A. (1995). On the spatial organization of soil moisture fields. *Geophysical Research Letters*, *22*(20), 2757–2760. https://doi.org/10.1029/95gl02779

Rosenbaum, U., Bogena, H. R., Herbst, M., Huisman, J. A., Peterson, T. J., Weuthen, A., et al. (2012). Seasonal and event dynamics of spatial soil moisture patterns at the small catchment scale. *Water Resources Research*, *48*(10), 2011WR011518. https://doi.org/10.1029/2011wr011518

Rötzer, K., Montzka, C., & Vereecken, H. (2015). Spatio-temporal variability of global soil moisture products. *Journal of Hydrology*, *522*, 187–202. https://doi.org/10.1016/j.jhydrol.2014.12.038

Rouholahnejad Freund, E., Fan, Y., & Kirchner, J. W. (2020). Global assessment of how averaging over spatial heterogeneity in precipitation and potential evapotranspiration affects modeled evapotranspiration rates. *Hydrology and Earth System Sciences*, *24*(4), 1927–1938. https://doi.org/10.5194/hess-24-1927-2020

Rouholahnejad Freund, E., & Kirchner, J. W. (2017). A BUDYKO framework for estimating how spatial heterogeneity and lateral moisture redistribution affect average evapotranspiration rates as seen from the atmosphere. *Hydrology and Earth System Sciences*, *21*(1), 217–233. https://doi.org/10.5194/hess-21-217-2017

Ryu, D., & Famiglietti, J. S. (2005). Characterization of footprint-scale surface soil moisture variability using Gaussian and beta distribution functions during the Southern Great Plains 1997 (SGP97) hydrology experiment. *Water Resources Research*, *41*(12). https://doi.org/10.1029/2004wr003835

Sadri, S., Pan, M., Wada, Y., Vergopolan, N., Sheffield, J., Famiglietti, J. S., et al. (2020). A global near-real-time soil moisture index monitor for food security using integrated SMOS and SMAP. *Remote Sensing of Environment*, *246*, 111864. https://doi.org/10.1016/j.rse.2020.111864

Simon, J. S., Bragg, A. D., Dirmeyer, P. A., & Chaney, N. W. (2021). Semi-coupling of a field-scale resolving land-surface model and WRF-LES to investigate the influence of land-surface heterogeneity on cloud development. *Journal of Advances in Modeling Earth Systems*, *13*(10). https://doi.org/10.1029/2021ms002602

Sivapalan, M., Beven, K., & Wood, E. F. (1987). On hydrologic similarity: 2. A scaled model of storm runoff production. *Water Resources Research*, *23*(12), 2266–2278. https://doi.org/10.1029/wr023i012p02266

Sylvain, Z. A., Wall, D. H., Cherwin, K. L., Peters, D. P. C., Reichmann, L. G., & Sala, O. E. (2014). Soil animal responses to moisture availability are largely scale, not ecosystem dependent: Insight from a cross-site study. *Global Change Biology*, *20*(8), 2631–2643. https://doi.org/10.1111/gcb.12522

Taufik, M., Torfs, P. J. J. F., Uijlenhoet, R., Jones, P. D., Murdiyarso, D., & Van Lanen, H. A. J. (2017). Amplification of wildfire area burnt by hydrological drought in the humid tropics. *Nature Climate Change*, *7*(6), 428–431. https://doi.org/10.1038/nclimate3280

Trugman, A. T., Medvigy, D., Mankin, J. S., & Anderegg, W. R. L. (2018). Soil moisture stress as a major driver of carbon cycle uncertainty. *Geophysical Research Letters*, *45*(13), 6495–6503. https://doi.org/10.1029/2018gl078131

Vereecken, H., Huisman, J., Pachepsky, Y., Montzka, C., van der Kruk, J., Bogena, H., et al. (2014). On the spatio-temporal dynamics of soil moisture at the field scale. *Journal of Hydrology*, *516*, 76–96. https://doi.org/10.1016/j.jhydrol.2013.11.061

Vergopolan, N., Chaney, N. W., Beck, H. E., Pan, M., Sheffield, J., Chan, S., & Wood, E. F. (2020). Combining hyper-resolution land surface modeling with smap brightness temperatures to obtain 30-m soil moisture estimates. *Remote Sensing of Environment*, *242*, 111740. https://doi.org/10.1016/j.rse.2020.111740

Vergopolan, N., Chaney, N. W., Pan, M., Sheffield, J., Beck, H. E., Ferguson, C. R., et al. (2021a). Smap-hydroblocks, a 30m satellite-based soil moisture dataset for the conterminous us. *Scientific Data*, *8*(1), 264. https://doi.org/10.1038/s41597021010502

Vergopolan, N., Chaney, N. W., Pan, M., Sheffield, J., Beck, H. E., Ferguson, C. R., et al. (2021b). Smap-hydroblocks: Hyper-resolution satellite-based soil moisture over the continental United States. *Zenodo*. https://doi.org/10.5281/zenodo.4441212

Vergopolan, N., & Fisher, J. B. (2016). The impact of deforestation on the hydrological cycle in amazonia as observed from remote sensing. *International Journal of Remote Sensing*, *37*(22), 5412–5430. https://doi.org/10.1080/01431161.2016.1232874

Vergopolan, N., Xiong, S., Estes, L., Wanders, N., Chaney, N. W., Wood, E. F., et al. (2021). Field-scale soil moisture bridges the spatial-scale gap between drought monitoring and agricultural yields. *Hydrology and Earth System Sciences*, *25*(4), 1827–1847. https://doi.org/10.5194/hess-25-1827-2021

Wall, D. H. (2013). *Soil ecology and ecosystem services*. Oxford University Press.

Wall, D. H., & Virginia, R. A. (1999). Controls on soil biodiversity: Insights from extreme environments. *Applied Soil Ecology*, *13*(2), 137–150. https://doi.org/10.1016/s0929-1393(99)00029-3

Wang, S., Zhang, K., van Beek, L. P., Tian, X., & Bogaard, T. A. (2020). Physically-based landslide prediction over a large region: Scaling low-resolution hydrological model results for high-resolution slope stability assessment. *Environmental Modelling & Software*, *124*, 104607. https://doi.org/10.1016/j.envsoft.2019.104607

Western, A. W., Grayson, R. B., Blöschl, G., & Wilson, D. J. (2003). *Spatial variability of soil moisture and its implications for scaling*. (pp. 119–142). CRC Press.

Youngquist, M. B., & Boone, M. D. (2014). Movement of amphibians through agricultural landscapes: The role of habitat on edge permeability. *Biological Conservation*, *175*, 148–155. https://doi.org/10.1016/j.biocon.2014.04.028

Zhang, J., van Westen, C. J., Tanyas, H., Mavrouli, O., Ge, Y., Bajrachary, S., et al. (2019). How size and trigger matter: Analyzing rainfall- and earthquake-triggered landslide inventories and their causal relation in the Koshi River basin, central Himalaya. *Natural Hazards and Earth System Sciences*, *19*(8), 1789–1805. https://doi.org/10.5194/nhess-19-1789-2019

Zheng, Y., Brunsell, N. A., Alfieri, J. G., & Niyogi, D. (2021). Impacts of land cover heterogeneity and land surface parameterizations on turbulent characteristics and mesoscale simulations. *Meteorology and Atmospheric Physics*, *133*(3), 589–610. https://doi.org/10.1007/s00703-020-00768-9

Zhu, Z., Wright, D. B., & Yu, G. (2018). The impact of rainfall space-time structure in flood frequency analysis. *Water Resources Research*, *54*(11), 8983–8998. https://doi.org/10.1029/2018wr023550

References From the Supporting Information

Chaney, N. W., Metcalfe, P., & Wood, E. F. (2016). Hydroblocks: A field-scale resolving land surface model for application over continental extents. *Hydrological Processes*, *30*(20), 3543–3559. https://doi.org/10.1002/hyp.10891

Chaney, N. W., Minasny, B., Herman, J. D., Nauman, T. W., Brungard, C. W., Morgan, C. L. S., et al. (2019). Polaris soil properties: 30-m probabilistic maps of soil properties over the contiguous United States. *Water Resources Research*, *55*(4), 2916–2938. https://doi.org/10.1029/2018wr022797

Danielson, J. J., & Gesch, D. B. (2011). *Global multi-resolution terrain elevation data 2010 (GMTED2010)*. US Department of the Interior, US Geological Survey.

Fick, S. E., & Hijmans, R. J. (2017). Worldclim 2: New 1-km spatial resolution climate surfaces for global land areas. *International Journal of Climatology*, *37*(12), 4302–4315. https://doi.org/10.1002/joc.5086

Homer, C. G., Dewitz, J., Yang, L., Jin, S., Danielson, P., Xian, G. Z., et al. (2011). Completion of the 2011 national land cover database for the conterminous United States – Representing a decade of land cover change information. *Photogrammetric Engineering and Remote Sensing*, *81*, 345–354. Retrieved from https://pubs.er.usgs.gov/publication/70146301

Ryu, D., & Famiglietti, J. S. (2006). Multi-scale spatial correlation and scaling behavior of surface soil moisture. *Geophysical Research Letters*, *33*(8), L08404. https://doi.org/10.1029/2006gl025831

Vanmarcke, E. (1984). *Random fields: Analysis and synthesis*. MIT Press.

Western, A. W., & Blöschl, G. (1999). On the spatial scaling of soil moisture. *Journal of Hydrology*, *217*(3–4), 203–224. https://doi.org/10.1016/s0022-1694(98)00232-7